

# Tip Clearance Effects on Performance of a Centrifugal Compressor

S. M. Swamy<sup>1</sup>

V.Pandurangadu<sup>2</sup>

1. Assistant Professor, Department of Mechanical Engineering, GNITS, Hyderabad.  
e-mail: moodswamy@yahoo.co.in

2. Professors, Department of Mechanical Engineering, JNTUCE, Anantapur.

**Abstract**-Tip clearance effects on flow field of a low speed centrifugal compressor performance is tested experimentally by using partial shroud (PS) attached to the rotor blade tip at three values of tip clearances i.e.= 2.2%, 5.1% and 7.9 % of blade height at trailing edge are examined at three flow coefficients 0.18, 0.28, and 0.34. The effect of tip clearance on total pressure coefficient and static pressure coefficient exit of the compressor is analyzed. The drop in static pressure coefficient and total pressure coefficient with increase in tip clearance is found to be high at the tip of the blade due to high pressure fluid leakage at the tip of the blade. Performance reduction with tip clearance is observed. The mass averaged total and static pressures at the rotor exit at the three values of tip clearances clearly show that partial shrouds are beneficial in improving the pressure rise of the compressor. This benefit is found to be more at the higher value of tip clearance tested.

**Keywords:** Compressor, tip clearance, partial shroud, ps on tip of the rotor blade, casing, tip leakage flow.

## Introduction:

The centrifugal compressors have a wide range of applications especially for power plants for small aircraft and helicopters, in process industries, compression of gases and vapours, because they can provide high-pressure ratios and large operating ranges with relatively high efficiencies. Centrifugal compressors are used primarily for their suitability for handling small volume flows, but other advantages include a shorter length than an equivalent axial flow compressor, less susceptibility to loss of performance by buildup of deposits on the blade surfaces and their suitability to operate over a wide range of mass flow. The efficiency of a centrifugal compressor is lower than that of an axial flow compressor. Efficiency is probably the most important performance parameter for turbo machines. The conditions of flow in the tip region of rotor blades are very complex, due to strong interaction of the leakage flow with the boundary layers and secondary flows. The tip leakage flow thus would have dominant effect on the performance of a compressor. Tip clearance in centrifugal compressor causes the leakage of high pressure fluid from pressure surface to suction surface of the impeller blade, making the flow field highly complex and effecting the performance. The required tip clearance can be obtained by shifting the casing in radial or axial or combined radial and axial directions. Hayami (1997) has found from his experiments that axial movement of the casing has better efficiency over the movement of casing in radial and axial directions. Radial movement of casing increases clearance at inducer, which reduces the operating range. The tip clearance studies are conducted to understand the flow behavior in order to minimise the effect of tip clearance. Pampreen (1973), Mashimo et al. (1979), Sitaram and Pandey (1990) have conducted experimental studies and suggested that by reducing the tip clearance gap size, the tip clearance effect can be minimised. The effect of tip leakage on flow behavior in rotating impeller passage was carried out by Hathaway et al. (1993). Farge et al. (1989) carried out the impeller passage measurements at five stations in a low speed centrifugal compressor using a five hole probe rotating with the impeller. A comprehensive review of tip clearance effects in centrifugal compressors is given by Pampreen (1983).

Senoo and Ishida (1987) gave analytical expression to quantify the tip clearance effects in centrifugal blowers. Senoo (1991) gave a comprehensive review of mechanics of tip leakage flows in axial and centrifugal compressors. Ishida et al. (1987) had tested centrifugal blowers with different shapes (square, round and E-type, i.e. with an extension on the pressure surface side) and found that E-type tip provided improved performance. Sitaram and Swamy (2011) had tested a centrifugal compressor with different types of passive means, viz. turbulence generator at different positions and partial shroud attached the rotor blade tip and found that the partial shroud gave improved performance at all the values of the tip clearance. Hence the present investigation is undertaken to further explore the reason for this improvements. The paper reports these measurements at three flow coefficients, namely  $\phi=0.18$  (below design flow coefficient),  $\phi=0.28$  (design flow coefficient) and  $\phi=0.34$  (above design flow coefficient).

**Experimental Facility:** The present experimental investigations are carried on a low speed centrifugal compressor set up. A schematic layout of the experimental set up is shown in Fig. 1. The experimental set up consists of essentially a centrifugal rotor driven by a 5 kW D.C. motor with a rated speed of 2000 rpm. The D.C. motor is directly coupled to the shaft carrying the rotor.

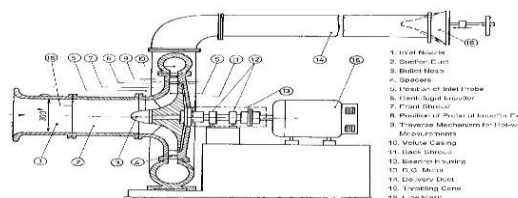


Fig. 1 Schematic diagram of centrifugal compressor setup

The main components of the compressor are suction duct, rotor, vaneless diffuser formed by the front and rear walls of the casing and volute casing of circular cross section and a delivery duct with a throttle at its outlet and nozzle at the inlet. The major design details of the compressor are given in Table 1.

Table 1 Design Details of the Rotor

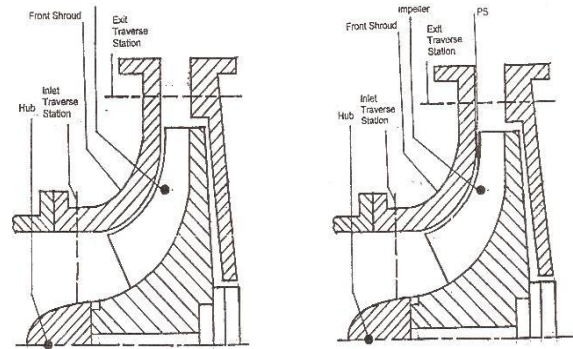
Total pressure rise, $\Delta p$ :	300 mm WG
Volume flow rate, $V$ :	1.12 m <sup>3</sup> /s
Speed of rotation, $N$ :	2000 rpm
Shape number, $N_{sh}$ :	0.092
No. of rotor blades, $Z$ :	16
Inducer hub diameter, $d_{ih}$ :	160 mm
Inducer tip diameter, $d_{it}$ :	300 mm
Rotor tip diameter, $d_2$ :	500 mm
Blade height at the exit, $h_2$ :	34.74 mm
Blade angle at inducer tip, $\beta_{it}$ :	35°
Blade angle inducer hub, $\beta_{ih}$ :	53°
Blade angle at exit, $\beta_2$ :	(a) At hub: 75° (b) At mean section: 90° (c) At tip: 105°
All the angles are measured w. r. t. tangential direction	

**Partial Shroud:** The partial shrouds are made of stainless steel of 0.1 mm thickness. The stainless steel sheet is cut to the shape of rectangle pieces of 50 mm x 5 mm size. These rectangle pieces are attached to the tip of the blades using araldite. The configurations tested (basic configuration without partial shroud and configuration with partial shroud) are shown in Fig. 2. The blade-to-blade view showing the partial shroud on the rotor tip is also shown in Fig. 2.

**Instrumentation:** The performance of the compressor is determined by the change in the static pressure across the compressor. The static pressures on the suction duct and delivery duct are measured using a scanning box (Model FC091-3) and micro manometer (model FCO12) manufactured by M/s Furness Control Ltd. The scanning box contained 20 valves, which are numbered sequentially. The pressures to be measured are connected to the numbered inputs. Pressure inputs are read in sequence by using the micro manometer. The micro manometer is a sensitive differential pressure measuring unit, capable of reading air pressures from 0.01 mm to 2000 mm WG. It would respond to pressure inputs up to 50 Hz. But the time constant potentiometer can be used to average the pressure fluctuations.

The speed of the centrifugal compressor is measured using a non-contact type digital tachometer. Four interconnected static pressure tappings on the inlet bell mouth casing wall at the throat section are used to determine the inlet velocity. Knowing the bellmouth area, the volume flow is calculated using a suitable value of coefficient of discharge for the bellmouth. A D.C. motor with a separate exciter drives the centrifugal compressor. The input power was measured by mean of voltmeters and ammeters connected separately for field and armature supplies. A suitable value of motor efficiency is used to get the rotor input power.

The static pressure on the diffuser is measured at the above values of tip clearances at three flow coefficients, viz.  $\phi=0.18$  (below design flow coefficient),  $\phi=0.28$  (design flow coefficient) and  $\phi=0.34$  (above design flow coefficient). A precalibrated five hole probe is used to measure the rotor exit flow at the three values of tip clearance and at the above three values of flow coefficient. The probe is calibrated at two velocities to estimate the effect of Reynolds number on the calibration and the effect is found to be small. The non-nulling method of Treaster and Yocum (1979) is used.



Basic Configuration

Configuration with PS

**Results and Discussion:**

**Performance Characteristics:** The results of the present investigation are presented and discussed in this section. The performance of the compressor in terms of  $\psi$  vs.  $\phi$  and  $\eta$  vs.  $\phi$  are presented. The non-dimensional parameters are defined as follows:

$$\text{Flow coefficient, } \phi = \frac{V}{\pi d_2 b_2 U_2} = \frac{C_{2r}}{U_2}$$

where  $V$  = Volume flow (m<sup>3</sup>/s)  
 $d_2$  = Rotor tip diameter (m)  
 $b_2$  = Rotor blade width at exit (m)

$c_{2r}$  = Radial velocity at rotor exit (m/s)  
 $U_2$  = Rotor tip speed (m/s)

$$\text{Energy coefficient, } \psi = \frac{2W}{U_2^2}$$

where  $W$  = Specific work (m<sup>2</sup>/s<sup>2</sup>)  

$$= \frac{p_d - p_s}{\rho} + \frac{c_2^2 - c_s^2}{2} + gZ$$

$$\text{Power coefficient, } \gamma = \frac{N_c}{\rho A U^3} = \frac{m}{\rho A U^2}$$

where  $N_c$  = Coupling power (Watts)  
 $A$  = Suction duct area (m<sup>2</sup>)  
 $E$  = Motor voltage (Volts)  
 $I$  = Motor current (Amps)  
 $\eta_m$  = Motor efficiency

$$\text{Compressor efficiency, } \eta_c = \frac{\rho \psi W}{\gamma}$$

Figure 3 shows the performance characteristic in terms of energy coefficient,  $\psi$  vs. flow coefficient,  $\phi$  for the three values of tip clearance for both configurations. At all values of tip clearance, PS gives higher value of energy coefficient, as the partial shroud obstructs the tip leakage flow and allows it to mix with main flow at a further distance. It may be observed that the performance of the rotor without PS at  $\tau=2.2\%$  is almost similar to that the rotor with PS at  $\tau=5.1\%$ . Hence by using partial shroud the rotor can operate at higher clearances with mechanical safe margins but without sacrificing performance. Figure 4 shows the performance characteristic in terms of efficiency,  $\eta$  vs. flow coefficient,  $\phi$  for the three values of tip clearance for both configurations. At all values of tip clearance, PS gives higher value of efficiency compared to that without PS due to reduced tip leakage flows. In fact the efficiency of the rotor with PS even at the highest value of tip clearance tested is higher than the efficiency of the rotor without partial shroud at the lowest value of tip clearance.

**Static pressure on casing:** The static pressure distribution on the casing for the three values of tip clearance at three flow coefficients for both configurations is shown in Fig. 6. On the casing, 8 nos. of static pressure taps are provided from the inducer leading edge to the rotor exit. The locations of the taps are shown as inset in Fig. 3. The casing has its inner contour shaped to match the rotor blade tip from the inlet to the exit of the rotor. The static pressure measurements on the casing give an indication of variation of the static pressure developed in the tip region of the rotor. The static pressure coefficient is defined as follows:

$$\psi_{ws} = 2 P_w / \rho U_2^2$$

From the figure it can be seen that the static pressure distribution is high for lower tip clearance when compared that at the higher tip clearance for all the flow coefficients. For the high flow coefficient considered, reduction in static pressure is higher near the inducer when compared to that at low flow coefficient. The pressure initially decreases due to suction and then uniformly increases, indicating that there is no dead zone or eddies near the casing region inside rotor and of the energy is transferred smoothly to the fluid near the casing.

**Rotor Exit Flow Measurements:**

**Total Pressure Coefficient,  $\psi_o$ :** The distribution of total pressure coefficient at the rotor exit for both configurations and three flow coefficients at the three values of tip clearances is shown in Fig. 7. The total pressure coefficient is defined as follows:

From the figure, it can be clearly seen that rotor with partial shroud (PS) shows increased total pressure coefficient, ( $\psi_o$ ) compared to basic configuration for all the flow coefficients at the tip clearance ( $\tau=2.2\%$ ). From the figure, it can be seen that the extent of region of improvement increases with reduction in flow coefficient. That means the higher the loading more is the benefit due to the partial shroud. For the tip clearance  $\tau=5.1\%$ , the benefits of PS are reduced. It can also be observed that, the total pressure coefficient increases as the flow coefficient decreases for all the tip clearances. For tip clearance  $\tau=7.9\%$  configuration with partial shroud also shows higher total pressure coefficient compared to basic configuration. This may be attributed to the partial shrouds attached to the tip of the blades restricting the tip leakage flow and hence increased total pressure is obtained. Trend of the total pressure coefficient is almost same for both configurations at three values of tip clearances.

**Static Pressure Coefficient,  $\psi_s$ :** The static pressure coefficient distribution at the rotor exit for two configurations and three flow coefficients for three values of tip clearances is shown in Fig. 8. The static pressure coefficient is defined as follows:

$$\psi_s = 2 P_s / \rho U_2^2$$

From the figure, it can be clearly seen that rotor with partial shroud (PS) shows increased static pressure coefficient, ( $\psi_s$ ) compared to basic configuration for all the flow coefficients at the three values of tip clearances ( $\tau=2.2\%$ ,  $5.1\%$  and  $7.9\%$ ). Similar to total pressure distribution, PS improves static pressure for a larger extent from the shroud, as the flow coefficient decreases. It can also be observed that, the static pressure coefficient is increasing as the flow coefficient increases for all the tip clearances. This may be attributed to the partial shrouds attached to the tip of the blades restricting the tip leakage flow. Trend of the static pressure coefficient is almost same for both configurations at three values of tip clearances. From the figure, it can be clearly seen that rotor with partial shroud (PS) shows increased total pressure coefficient, ( $\psi_o$ ) compared to basic configuration for all the flow coefficients at the tip clearance ( $\tau=2.2\%$ ). From the figure, it can be seen that the extent of region of improvement increases with reduction in flow coefficient. That means the higher the loading more is the benefit due to the partial shroud. For the tip clearance  $\tau=5.1\%$ , the benefits of PS are reduced. It can also be observed that, the total pressure coefficient increases as the flow coefficient decreases for all the tip clearances. For tip clearance  $\tau=7.9\%$  configuration with partial shroud also shows higher total pressure coefficient compared to basic configuration. This may be attributed to the partial shrouds attached to the tip of the blades restricting the tip leakage flow and hence increased total pressure is obtained. Trend of the total pressure coefficient is almost same for both configurations at three values of tip clearances. **Absolute Velocity,  $c$ :** is the axial distribution of non-dimensional absolute velocity at the rotor exit for two configurations and three flow coefficients for three values of tip clearances. Velocity and its radial and tangential components are non-dimensionalized with the rotor tip speed. From the figure, it can be seen that the absolute velocity increases with flow coefficient for all the tip clearances. For the three values of tip clearances at two flow coefficients ( $\phi=0.34$  and  $0.28$ ) clearly indicates an increase in absolute velocity in the rotor shroud region for the configuration with partial shroud, compared to the basic configuration. This is due to increase in tangential velocity, which means increased energy transfer. At flow coefficient ( $\phi=0.34$ ) an increase in absolute velocity is seen in the rotor hub region for the configuration with partial shroud, compared to the basic configuration. Trend of the absolute velocity is almost same for both configurations at three values of tip clearances. A careful study of this figure shows that basic configuration give lower absolute velocity for all the flow coefficients and for the three values of tip clearances. This lower absolute velocity is due to leakage flow in the flow field, which mixes with the main flow at the exit, resulting in lower values of velocities. **Radial Velocity,  $c_r$ :** is the distribution of non-dimensional radial velocity at the rotor exit for three flow coefficients and two rotor configurations for three values of tip clearances. For three values of tip clearances, it can be seen that radial velocity increased at flow coefficients ( $\phi=0.34$  and  $0.28$ ) in the rotor shroud region for the configuration with partial shroud, compared to the basic configuration. It can be observed

from the figures that at the shroud region for three values of flow coefficients show decrease in radial velocity for hub region. At shroud region, boundary layer thickness increases due to partial shroud. Therefore higher loading on the blade causes decrease in radial velocity in the hub region. *Tangential Velocity,  $c_u$*  is the axial distribution of non-dimensional tangential velocity for the three flow coefficients and for both configurations, and for three values of tip clearances at the rotor exit. From the figure, it can be clearly shown that configuration with partial shroud increases tangential velocity for two flow coefficients ( $\phi=0.34$  and  $0.28$ ) compared to the basic configuration of rotor. But at flow coefficient ( $\phi=0.18$ ), configuration with partial shroud shows increased tangential velocity for hub region. Also the trend of tangential velocity is almost same for both configurations at the three values of flow coefficients.

**Mass Averaged Performance of the Compressor:**

Mass averaged performance of compressor (Fig. 5) shows the variation of mass averaged values of total pressure coefficient ( $\psi_{O2}$ ) and static pressure coefficient ( $\psi_{S2}$ ) with flow coefficient. The mass averaged values are defined as follows:

$$\overline{\psi_{O2}} = \int \psi_{O2} c_{ho} dx / \int c_{ho} dx \quad \text{sl.} \quad \overline{\psi_{S2}} = \int \psi_{S2} c_{hr} dx / \int c_{hr} dx$$

The mass averaged values of total pressure coefficient and static pressure coefficient at the rotor exit for both configurations at the three values of tip clearances clearly show that partial shrouds are beneficial in improving the pressure rise of the compressor, compared to the basic configuration. It can also be observed that the mass averaged values of total pressure coefficient and static pressure coefficient at the rotor exit for both configurations at the three values of tip clearances, increasing as the flow coefficient decreases. Also mass averaged values decrease with increase in tip clearance. From the figure, partial shrouds are found to have more beneficial effects at higher values of tip clearance.

**CONCLUSIONS:**

The following major conclusions are drawn from the present investigation.

1. Configurations with partial shroud (PS) shows higher energy coefficient and efficiency compared to the basic configuration at all the values of tip clearance.
2. Basic configuration at  $\tau=7.9\%$  gives poor performance i.e. reduced operating range, reduced energy coefficient and efficiency over the entire operating range. Partial shrouds have beneficial effects in increasing energy coefficient and efficiency of compressor.
3. Radial velocity at the exit of rotor almost remains constant from hub to shroud for all the configurations and flow coefficients.
4. The tangential velocity at rotor exit decreases with increase in flow coefficient and this difference is reduced with decreasing flow coefficient.
5. The mass averaged total pressure coefficient and static pressure coefficients are higher for configuration with Sitaram, N. and Pandey, B. (1990) "Tip Clearance Effects on a Centrifugal Compressor", J. of the Aero. Society of India, **42** (2) 309-315.

partial shroud (PS) compared to basic configuration. The possible reason may be due to reduction in the detrimental effects of the tip clearance flows by the partial shroud. Partial shrouds have more beneficial effects at higher values of tip clearance.

**NOMENCLATURE**

b	Distance between the shroud and hub at the rotor exit (m)
$C_d$	Velocity in delivery duct (m/s)
$C_s$	Velocity in suction duct (m/s)
d	Rotor diameter (m)
N	Rotational speed of rotor (rpm)
$N_c$	Coupling power (Watt)
$N_{sh}$	Shape number = $N\sqrt{V/W^{3/4}}$
$P_s$	Static pressure (Pa)
$P_o$	Total pressure (Pa)
$p_d$	Delivery pressure (Pa)
$p_s$	Suction pressure (Pa)
t	Clearance of the rotor blade (m)
$U_2$	Rotor tip speed = $(\pi d_2 N/60)$ (m/s)
V	Volume flow rate ( $m^3/s$ )
W	Specific work ( $m^2/s^2$ )
$\phi$	Flow coefficient (defined in the text)
$\gamma$	Power coefficient
$\eta$	Efficiency (defined in the text)
$\psi$	Energy coefficient (defined in the text)

$\psi_o$  Total pressure coefficient =  $2P_o / U_2^2$

$\psi_s$  Static pressure coefficient =  $2P_s / U_2^2$

$\rho$  Density of air ( $kg/m^3$ )

$\tau$  Relative tip clearance =  $(t/b_2)$

**Superscript**

- Mass averaged value

**Subscript**

2 Tip

**REFERENCES**

Ishida, M. and Y. Senoo, (1981) On the Pressure Losses due to the Tip Clearance of Centrifugal Blowers, Trans. ASME J. of Engg. for Power, **103**(2) 271-278.

Ishida, M., Ueki, H. and Senoo, Y., 1990, "Effect of blade tip configuration on tip clearance loss of a centrifugal blower", ASME J. Turbo., **112**(1) 14-18.

Pampreen, R. C., (1983) "Small Turbomachinery Compressor and Fan Aerodynamics", ASME J. of Engg. for Power, **105**(2), 251-256.

Schumann, L. F., Clark, D. A. and Wood, J. R. (1987) "Effect of Area Ratio on the Performance of a 5.5:1 Pressure Ratio Centrifugal Impeller", ASME J. of Turbo., **109**(1) 10-19.

Senoo, Y., (1991) "Mechanics on the Tip Clearance Loss of Impeller Blades", ASME J. of Turbo., **113** (3), 581-597.

Senoo, Y. and Ishida, M. (1987) "Deterioration of Compressor Performance due to Tip Clearance of Centrifugal Impellers", ASME J. of Turbo., **109** (1), 55-61.

Treaster, A. L. and Yocum, A. M. (1979) "The calibration and application of five-hole probes", Trans. of ISA, **18**(3), 23-34.

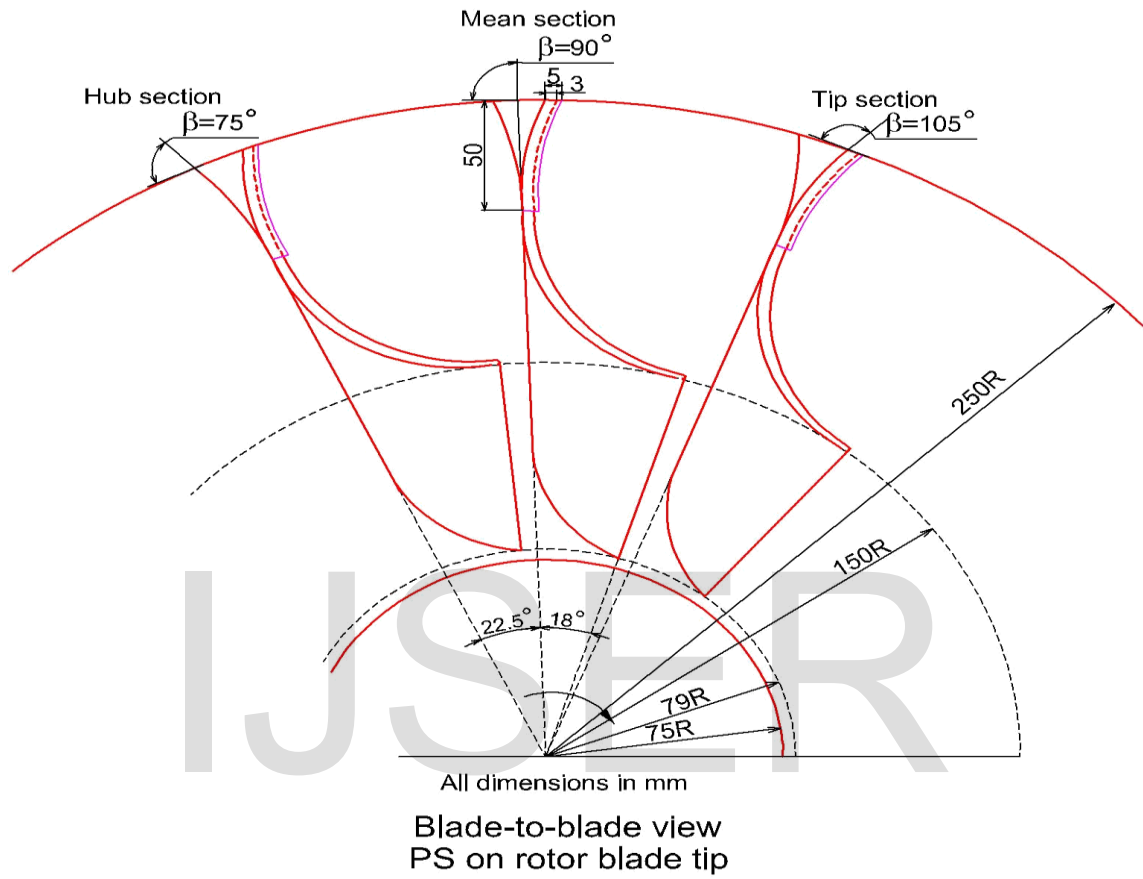


Fig.2 Details of Configurations Tested

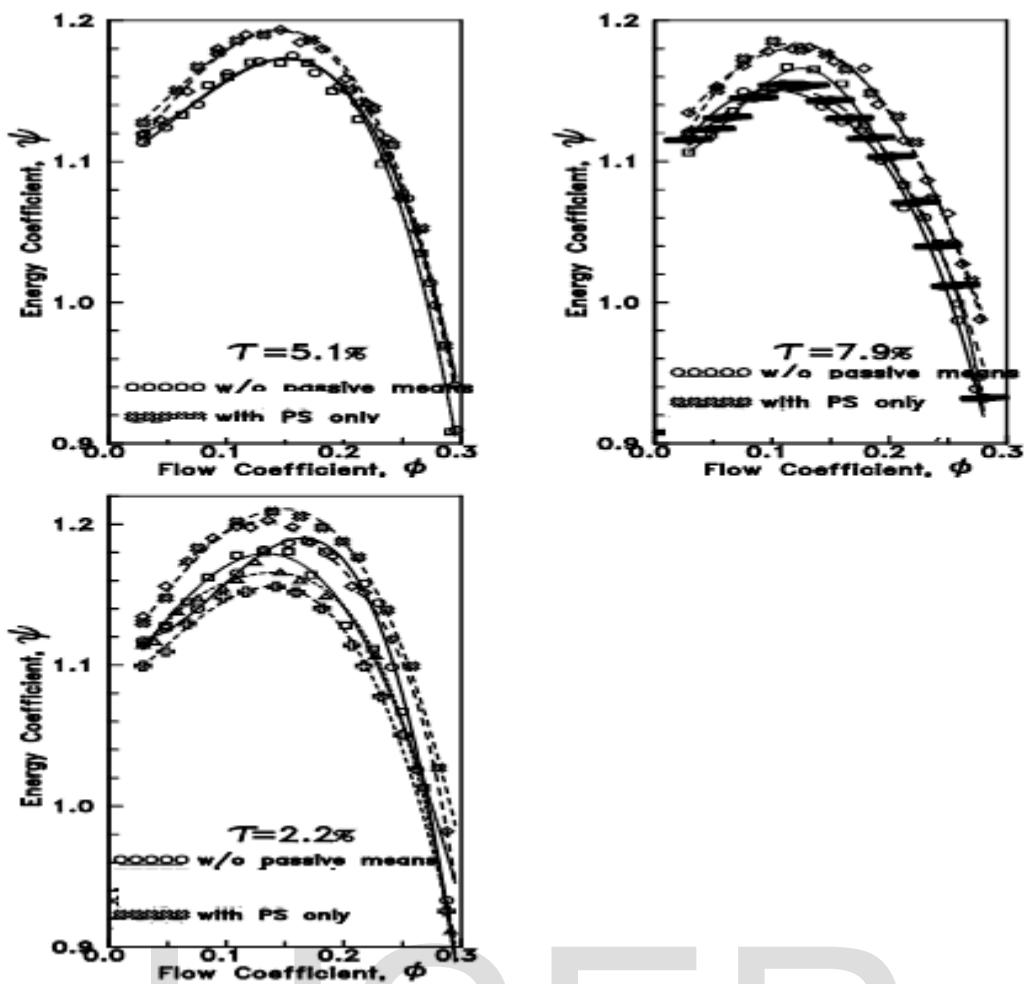


Fig.3 Performance of the centrifugal compressor: Energy coefficient vs. Flow coefficient

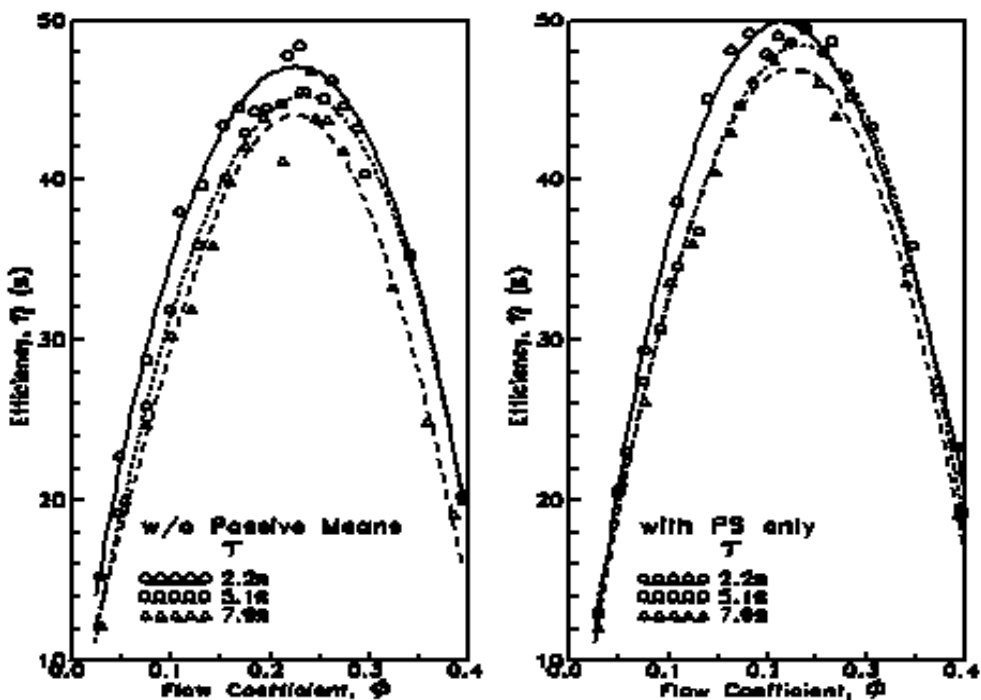


Fig 5 Performance Characteristics of Centrifugal Compressor (Efficiency,  $\eta$  vs. Flow Coefficient,  $\phi$ ) Effect of Tip Clearance

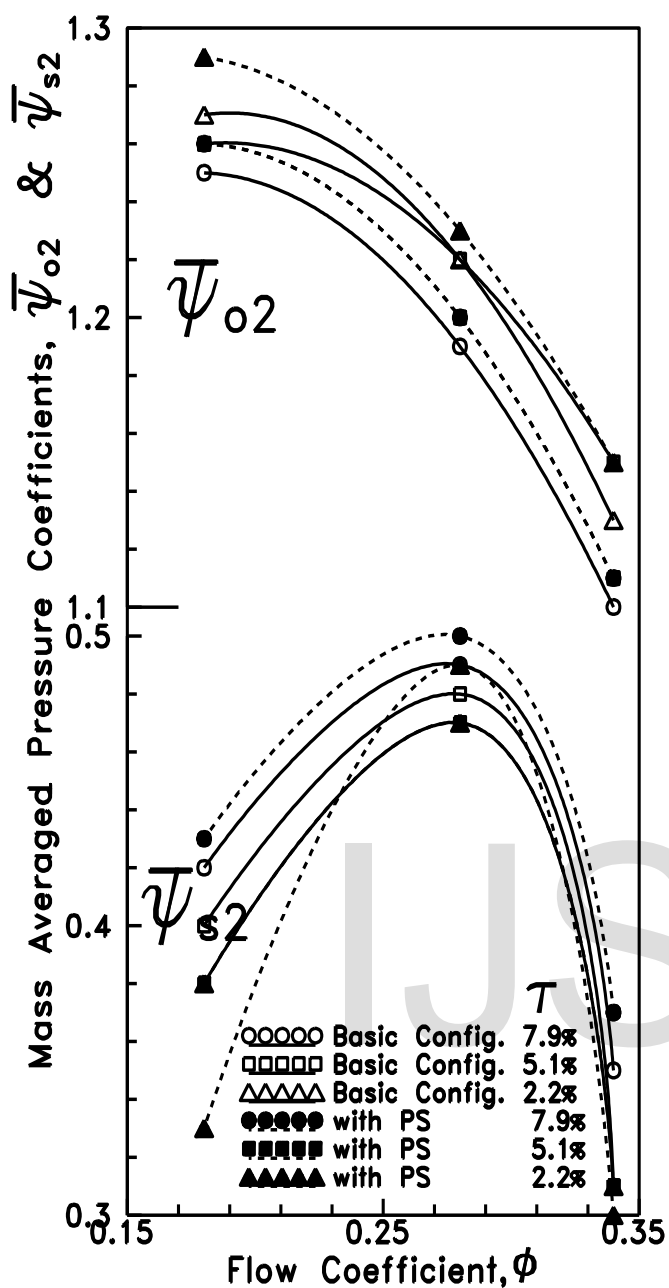


Fig.5 Mass averaged performance of the rotor

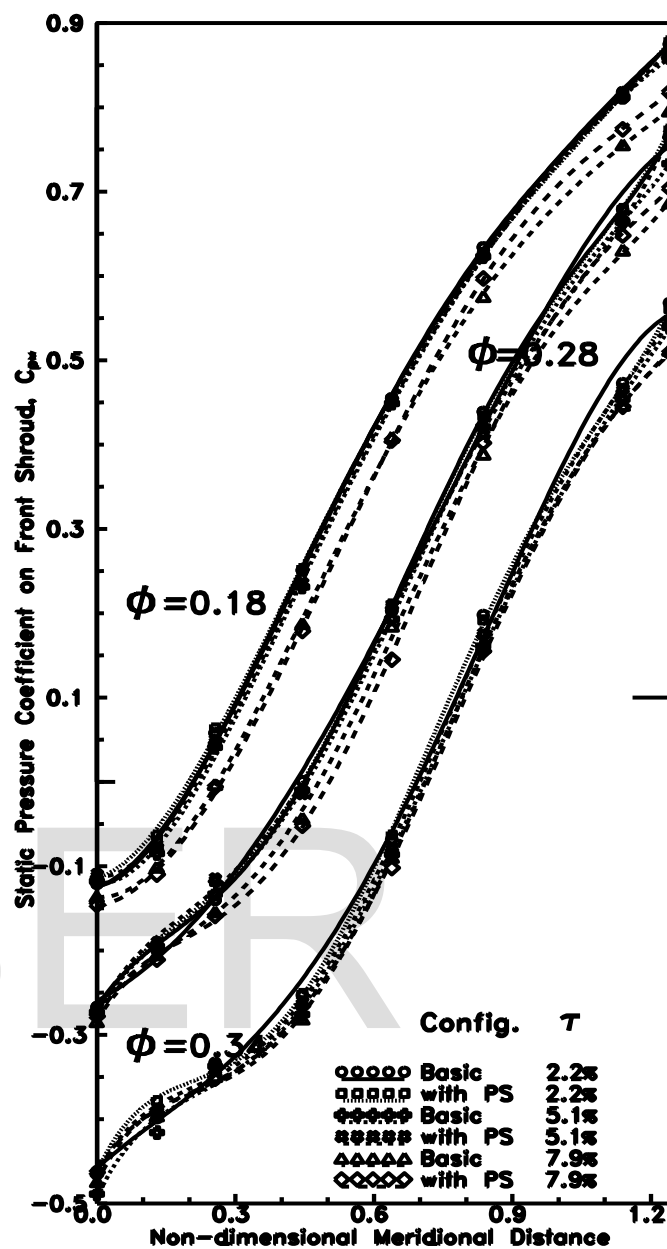


Fig.6 Distribution of static pressure on the casing

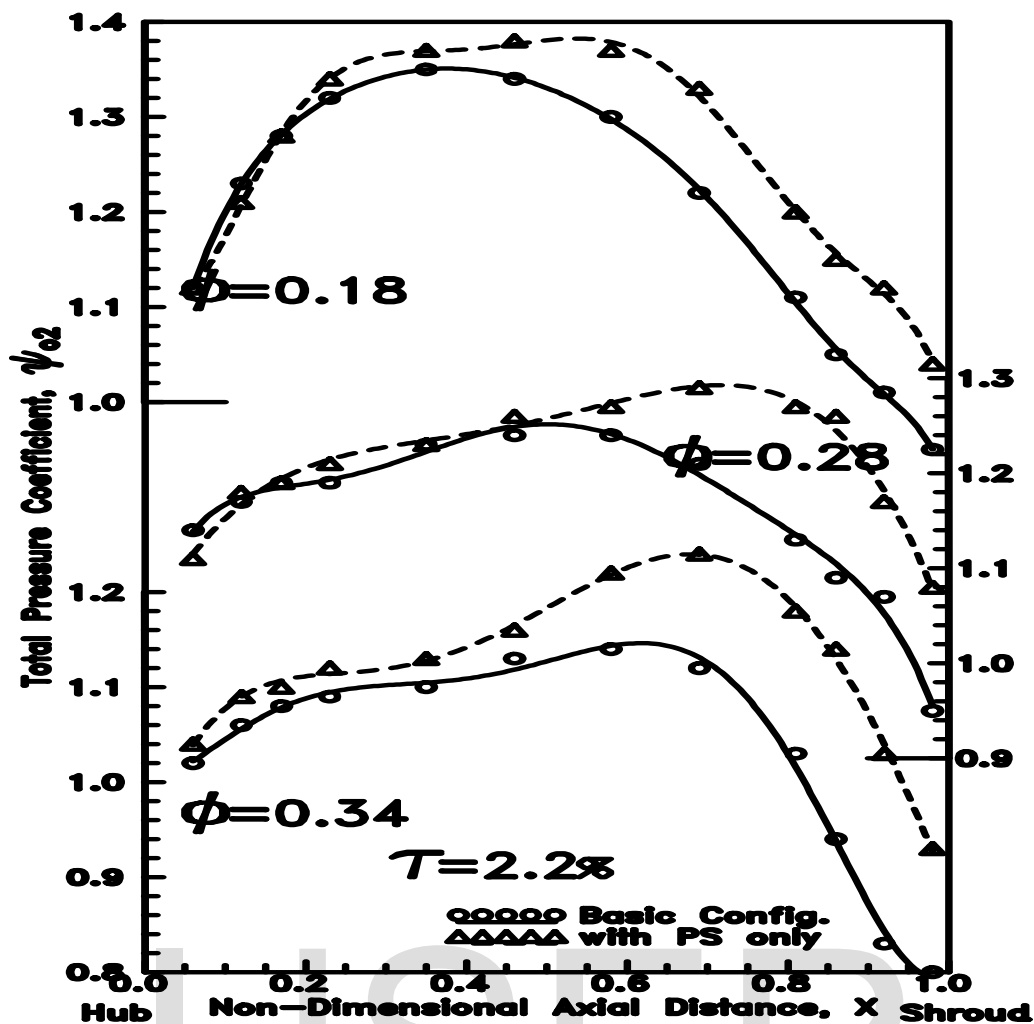


Fig.7 Distribution of total pressure coefficient at the rotor exit

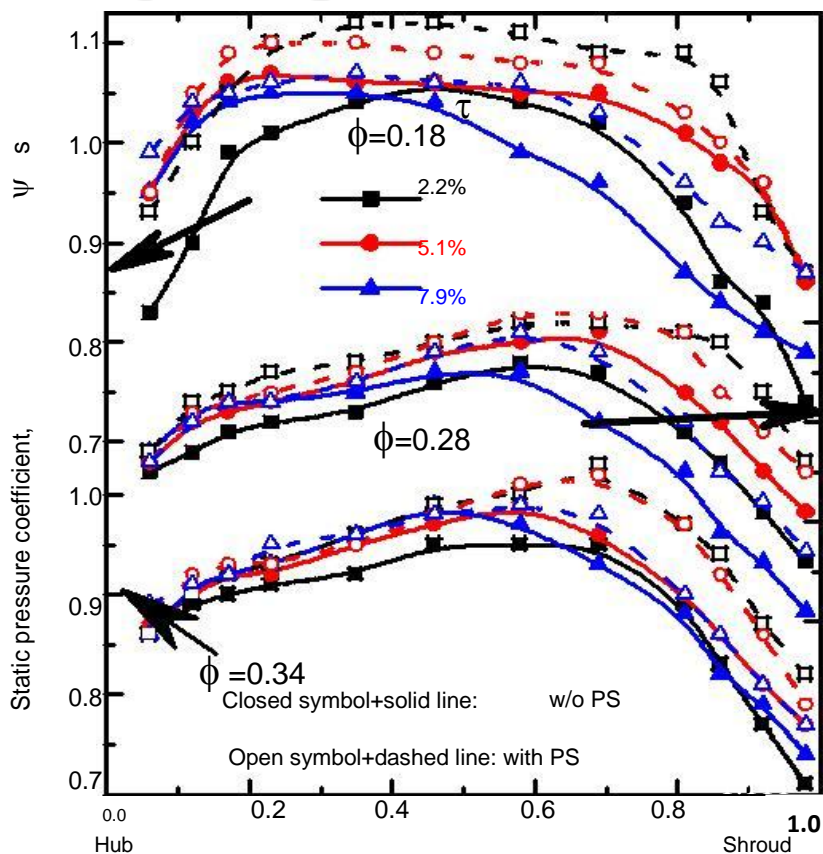


Fig.8 Distribution of static pressure coefficient at the rotor exit